Annihilation Gamma Ray Background Characterization and Rejection for a Positron Camera

Craig S. Levin, Martin P. Tornai, Lawrence R. MacDonald and Edward J. Hoffman

Division of Nuclear Medicine and Biophysics, UCLA School of Medicine
Los Angeles, CA 90095-6948

Abstract

We have developed a miniature (1.2 cm^2) beta-ray camera prototype to assist a surgeon in locating and removing the margins of a resected tumor. When imaging positron emitting radiopharmaceuticals, annihilation gamma ray interactions in the detector can mimic those of the betas. The extent of the background contamination depends on the detector, geometry and tumor specificity of the radiopharmaceutical. We have characterized the effects that annihilation gamma rays have on positron imaging with the camera. We studied beta and gamma ray detection rates and imaging using small positron or electron sources directly exposed to the detector to simulate hot tumor remnants and a cylinder filled with ^{18}F to simulate annihilation background from the brain. For various ratios of phantom brain/tumor activity, a annihilation gamma rate of 1.8 cts/sec/μCi was measured in the $CaF_2(Eu)$ detector. We present two gamma-ray background rejection schemes that use a β–γ coincidence. Results show that the coincidence methods works with ~99% gamma ray rejection efficiency.

I. INTRODUCTION

We have developed [1-8] miniature (≤1.2 cm^2), gamma (γ) and beta (β) ray imaging scintillation camera prototypes for the purpose of assisting a surgeon in locating and removing the margins of a resected tumor. The β imaging device directly detects positrons or electrons emitted from radiolabeled tissue exposed during surgery. The short range of the β's in tissue and detector and close proximity imaging of the activity (lesion) ensure high sensitivity and resolution and no need for a collimator. Imaging capabilities *in situ* help to distinguish signal from background and allow a relatively large area to be assayed in a relatively short time. Most of the pure β emitting radiopharmaceuticals readily available and used in the nuclear medicine clinic for tumor imaging are positron emitters (usually ^{18}F-labeled) for Positron Emission Tomography (PET). Using positron emitters, the detector will measure activity from annihilation γ rays (background) as well as from positrons (signal). The ability to extract the true β activity image from the total β and background γ signal depends on the ratio of tumor to background γ ray activity rates observed. This, in turn, depends on the radiopharmaceutical tumor uptake specificity. A candidate radiopharmaceutical for use in conjunction with this surgical probe is ^{18}F-Fluorodeoxyuridine (FdUr). PET studies with this tracer have shown brain tumor to normal tissue uptake ratios as high as 12:1.

A few techniques have been proposed for gamma ray background (GRB) rejection for non-imaging intraoperative β probes detecting positrons [9,10]. In this work we propose two new "on-line" background rejection schemes for an imaging device, both of which use beta-gamma (β–γ) coincidence detection. GRB rejection is achieved by requiring a detected coincidence between $CaF_2(Eu)$, the primary β detector, and an adjacent secondary detector that detects the associated γ ray. We will demonstrate the method using ^{18}F, a positron emitter used as a label for tumor detection in PET. With positrons there are two associated γ rays associated with each β event detected. The β-γ coincidence GRB rejection scheme is especially useful for positron annihilation GRB removal. Since two γ rays are emitted roughly 180° apart this ensures a high geometric efficiency for detection of at least one. However, this GRB rejection technique could, in principle, be useful for any β-emitting pharmaceutical (such as ^{131}I) that has accompanying GRB present (with a lower sensitivity compared to ^{18}F results: only one γ ray is emitted).

II. METHODS

The intricate details of the imaging device used are described elsewhere [5]. Fiber optics read out the scintillation light from a 1.25 cm diameter $CaF_2(Eu)$ disk and guide it to a multi-channel photo-multiplier tube (MCPMT). The fiber optic readout cabling provides flexibility for the surgeon and isolates exposed tissue from the bulky MCPMT, electronics, and high voltage distributions. The MCPMT tube is read out into 4 signals (x_+, x_-, y_+, y_-) using resistive charge division and the detected events are positioned with the standard logic. The intrinsic resolution of the device is 0.5 mm FWHM. A near-by cylindrical Lucite phantom (16 cm dia., 4 cm high) filled with ^{18}F simulates the head γ ray activity distribution. A small ^{204}Tl (β^-, E_{max}=765 keV, $\tau_{1/2}$=3.8 yr) or ^{18}F (β^+, E_{max}=635 keV, $\tau_{1/2}$=110 min) source, taped on the bottom of the cylinder, simulates the tumor site/surgical cavity activity.

For background considerations, we want the detector to be as thin as possible, yet thick enough to stop a majority of the β's (for higher light output and sensitivity). A $CaF_2(Eu)$ thickness of ~0.5-0.7 mm is optimal (Z_{eff} = 16.9, ρ = 3.17 g/cm^3) for low γ- and high β-ray detection efficiencies [4]. For all measurements, the β and γ ray components of the total activity are determined by using the "β shield" method. The contribution solely due to γ rays was measured by placing a plastic β shield between the β source and the scintillator. The β activity is obtained by subtracting the decay corrected γ component from the total γ+β signal, The plastic β shield used was 5 mm thick. For $CaF_2(Eu)$ thickness < 1.6 mm, ^{18}F flood irradiation studies showed both the γ and γ/β activity to roughly increase roughly linearly with thickness.

Two experiments were performed to ascertain the effects of GRB on β ray detection and imaging. In the first measurement, the ^{204}Tl source (fixed activity for the duration of the experiment) was used to simulate the residual tumor activity. The source was collimated in a 2 mm spot on the center of a 0.8 mm thick $CaF_2(Eu)$ disk with a collimated activity of approximately 60 nCi. An initial activity of approximately 1 mCi of ^{18}F was placed in the cylindrical head phantom with volume of roughly 800 cm^3. The total activity was measured as the ^{18}F decayed away with time. This experiment is useful since it demonstrates the effects of GRB for various ratios of detected γ/β rates.

The second experiment utilized the U-C-L-A #1 copper β transmission phantom [5] (see top of Fig. 4) to characterize the effects of GRB on imaging. The β phantom lettering is composed of 0.5 mm holes drilled in 0.4 mm thick copper, spaced 0.6 mm apart. The copper mask was placed directly on top of the detector The cylindrical phantom, filled with ^{18}F was placed 3 cm from the top of the imaging probe and mask.

0-7803-3534-1/97 10.00©1997IEEE

Figure 1 depicts two "on-line" annihilation GRB rejection techniques we have investigated, both of which utilize the β^+-γ coincidence technique. Requiring a hit from a positron in the $CaF_2(Eu)$ in coincidence with a hit from associated annihilation γ ray in a nearby detector, will allow us to separate true positron events from background. *The "gamma annulus"* approach utilizes a secondary scintillator (shielded from direct β interactions, and efficient for γ rays) that completely surrounds the front end of the imaging probe. With this geometry, at least one of the two back-to-back annihilation γ rays resulting from a positron stopping in the $CaF_2(Eu)$ will have a good chance of interacting with the annulus no matter where the positron annihilation occurs within the $CaF_2(Eu)$. In principal, for a very long annulus surrounding the detector, this would imply 4π coverage (only 2π coverage is required to detect at least one from the pair). The event will be recorded as a true positron event only if there is a coincidence between the two detectors. The U-C-L-A letter transmission phantom was used to determine the efficiency of this background rejection scheme. Another process that could mimic this dual hit signature would be a Compton scatter in the $CaF_2(Eu)$ followed by a photoabsorption in the γ ray detector. This secondary process is unlikely since there are two γ-ray interactions required (one in a low density, low Z material), compared to only one for the desired -γ event (β^+ will always interact in the $CaF_2(Eu)$).

The "phoswich" approach , uses a γ ray efficient detector (assume GSO, for example) that is both much faster than $CaF_2(Eu)$, and is transparent to its blue scintillation light. This scintillator is "sandwiched" between the $CaF_2(Eu)$ and the fiber bundle. The GSO serves the dual purpose of the fast γ-ray detector and the light diffuser required for the continuous $CaF_2(Eu)$ scintillator imaging [4,5]. In the phoswich configuration, the differences in both decay time and light output between the $CaF_2(Eu)$ (slow decay ~1 μs) and the GSO (fast decay, 60 ns) allows one to use pulse shape discrimination methods to identify the coincident events of interest. The events are clearly distinguishable because the decay times of the two scintillators differ by more than a factor of 10. An annihilation γ ray associated with the positron of interest will very likely traverse the secondary detector and a good event will have a signature of two added pulses: one slow ($CaF_2(Eu)$) and one fast (GSO). By triggering on the rise of the fast decay portion of the signal, delaying by the decay time of that pulse (typically <100 ns), and then integrating the slow portion of the pulse, nearly 90% of the true positron signal will be extracted. This is accomplished with the use of a fast leading edge or constant fraction discriminator, set above the $CaF_2(Eu)$ amplitudes, to trigger a linear gate for the amplified positioning signals of the imaging probe. The linear gate is normally closed and will open with a delayed signal from the γ ray detector trigger. The more efficient, faster and higher light yield the second detector, the better this technique works.

As for any background rejection scheme, the β^+-γ coincidence method results in an overall reduction in sensitivity. The extent of reduction depends on the detection efficiency of the γ ray detector. In principal, if that detector has a high stopping power for 511 keV γ rays and subtends a large solid angle in the "downward" direction (see Fig. 1) for all positions within the $CaF_2(Eu)$, the coincident sensitivity of the system will be acceptable.

For both β^+-γ coincidence rejection schemes investigated, the efficiency of the γ ray rejection can be measured by comparing the detected γ/β ratio with and without the β^+-γ coincidence. In addition, if we block the β's during coincidence acquisition, the resulting events seen are due to the background γ–γ process (for example, a Compton scatter in the $CaF_2(Eu)$ followed by a photoabsorption in the adjacent γ ray detector).

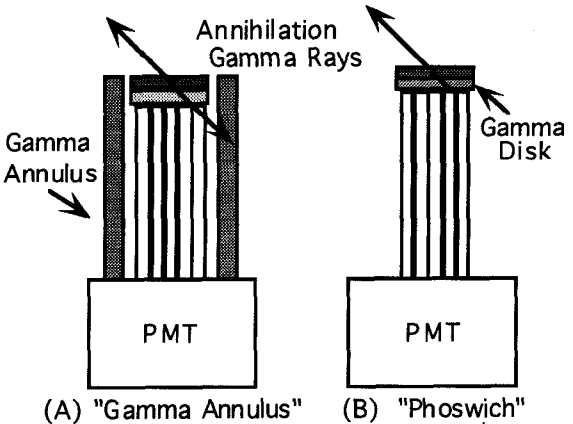

Figure 1. Schematic of two on-line β^+-γ coincidence annihilation background rejection techniques (a) the "gamma annulus" approach (b) The "phoswich" approach.

The number of coincident events measured with the β absorber in place compared to that without, when the two data sets are acquired for the same amount of time (with decay correction), determines how often two γ ray interactions mimic a β^+-γ event.

III. RESULTS

A. Detected Beta and Annihilation Gamma Ray Activity Rates

Figure 2 shows $\gamma+\beta$, γ and β spectra measured for 5 different ^{18}F phantom activity levels as it decays with time with an attached ^{204}Tl source of electrons (the $CaF_2(Eu)$ was not directly exposed to ^{18}F positrons). We see that even for this very thin $CaF_2(Eu)$ disk used (0.8 mm thick, 1.25 diameter) that the GRB detection rate is significant. For the first three spectra shown, the γ component dominates the measured activity. As the activity in the phantom decays, the constant ^{204}Tl electron activity (beta spectrum) emerges.

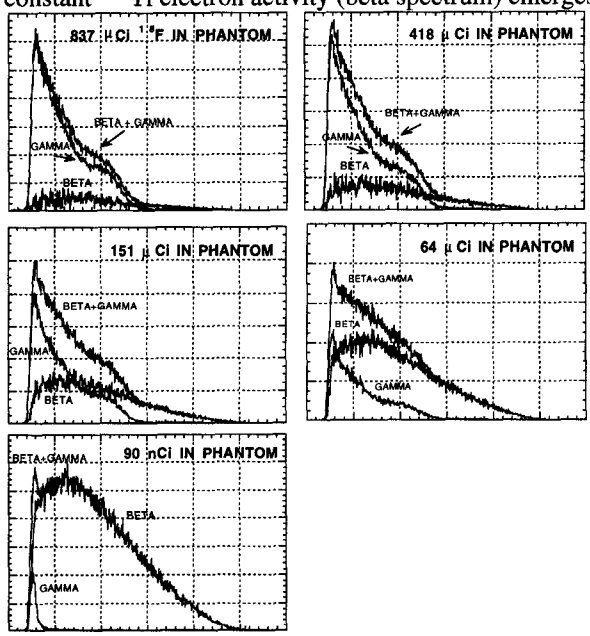

Figure 2. Some $\gamma+\beta$, γ and β activities measured for various ^{18}F phantom activity levels (with attached ^{204}Tl source). See Fig. 3.

Figure 3 displays the annihilation γ ray (from ^{18}F phantom, simulating head activity) and electron (collimated ^{204}Tl, simulating residual tumor activity) rates ratio measured

in the $CaF_2(Eu)$ as a function of head phantom ^{18}F activity. As expected, the β rate is constant and the γ rate varies linearly with phantom activity. A γ rate of 1.8 cts/sec/μCi from the phantom was measured. For this measurement, the activity from the collimated ^{204}Tl β source corresponded to approximately 60 nCi which yielded a constant detected β activity rate of roughly 4500 cts/sec/μCi from the ^{204}Tl source. However, for accurate positron imaging during surgery what matters is the ratio of the γ and β rates, not the absolute rates. Depending on the tumor affinity of the tracer used, the actual γ/β detected rate ratio expected for a tumor will lie somewhere on the line of Figure 3. For example, assume for the moment the 800 g cylinder properly estimates the mass of the brain and the 60 nCi β source roughly simulates a 10 mg piece of residual tumor. A 10:1 tumor (β source) to head (cylinder) uptake by volume (e.g. using FdUr) implies ~480 μCi in the head (cylinder). From Figure 3, this implies an expected activity γ/β rate ratio of approximately 3:1, which means some sort of GRB rejection scheme may be necessary. To reiterate, the relative, rather than absolute, residual tumor to head/tumor activity levels is what matters. For lower tumor to tissue uptake ratios the GRB problem will be worse.

We also measured the ratio of detected γ to β rates as a function of several values of ^{18}F point source (simulated tumor) activity values. Again the ^{18}F phantom simulated activity from the brain. With the given detector geometry and tumor model, the extent of GRB contamination can be determined from these measurements, once the brain to tumor activity is known. For example, a simulated head/tumor activity ratio of 4:1 implies that the detected γ/β ratio is approximately 1:1. The measured γ rate was 2.0 cts/sec/μCi, which compares well with that obtained with ^{204}Tl.

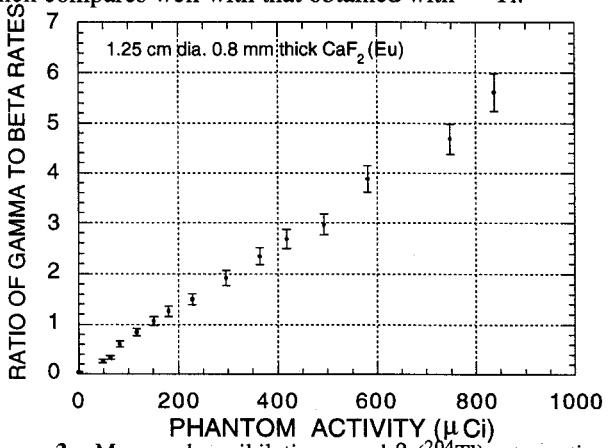

Figure 3. Measured annihilation γ and β (^{204}Tl) rates ratio as a function of head phantom ^{18}F activity. The collimated ^{204}Tl β source corresponded to approximately 60 nCi.

B. Effect of Annihilation Gamma Rays on Beta Imaging

Figure 4 demonstrates the potential problem of annihilation GRB for β imaging with this camera. Images were obtained using the U-C-L-A #1 copper transmission phantom (shown at top) on the β imaging probe irradiated with 100μCi of either ^{204}Tl (electrons, left image) or ^{18}F (positrons, right). The ^{18}F image shown was acquired with no activity in the brain phantom so it represents the best case scenario in terms of GRB. The potential need for annihilation background rejection is evident. The presence of positron annihilation GRB generated within the cotton swab, and/or the $CaF_2(Eu)$ is evident as a loss of contrast in the right compared to the left (pure β) image. The energy spectra of the particle components forming the images are shown below each image.

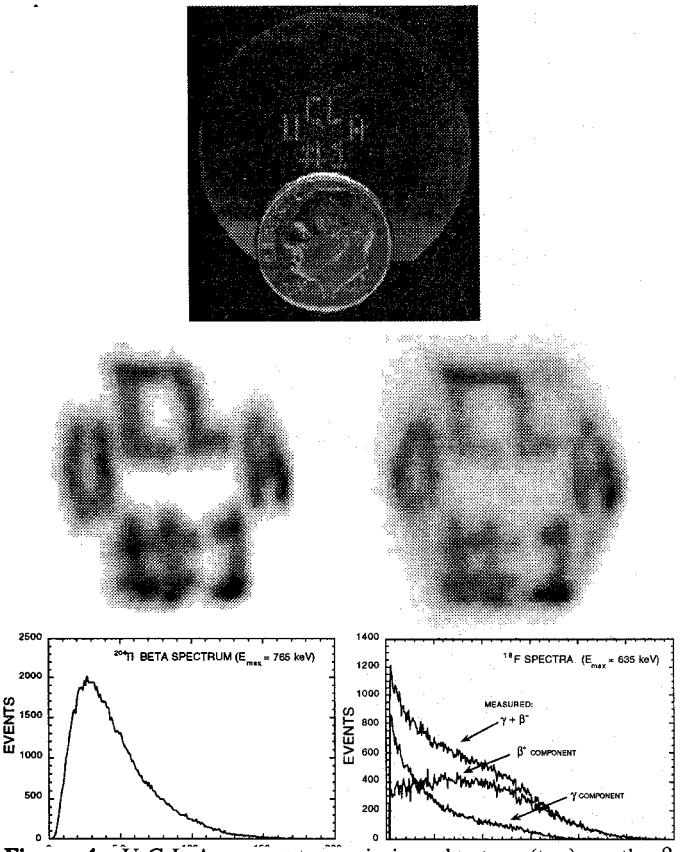

Figure 4. U-C-L-A copper transmission phantom (top) on the β imaging probe irradiated with either ^{204}Tl (electrons, left image) or ^{18}F (positrons, right image). Note loss of contrast in right image. The corresponding electron or positron, γ and combined spectra are shown beneath each image.

Again, the extent of GRB contamination depends on the tumor-seeking radio-pharmaceutical specificity. High specificity minimizes GRB.

Figure 5 (left three figures) demonstrates the "gold standard" for γ-ray background rejection which is achieved with the use of a positron "shield". The activity passing through the copper UCLA positron transmission phantom was consistent with a 3% tumor/tissue uptake ratio. We used this activity ratio because it was consistent with an analysis of previous UCLA FdUr PET studies of tumor uptake in the brain. This ratio underestimates the true γ/β activity ratio we would measure with our device since tumor self-absorption of betas was not taken into account. The left image shows the result for this realistic positron to γ ray source ratio with no shield present (positrons + γ rays). The second image shows the positron shielded result (only γ-rays). The third image shows that obtained by subtracting the γ-ray only component from the unshielded image (β only). Note the improvement in contrast seen after subtraction. The various energy spectra (γ+β, γ and β) are shown underneath each image. Unfortunately, it may not be possible for a surgeon using this imaging device to either insert a β shield or hold the device long enough to make two images. An on-line background rejection scheme would be preferable.

C. On-Line Annihilation Background Rejection Using β–γ Coincidence

On the far right of Figure 5 we show an imaging result obtained with the on-line β–γ coincidence background rejection method. This is shown in the same figure as the "gold standard", β-shield method for background removal (left 3

figures) for easy comparison. The "on-line' background rejection result was obtained from a prototype of the "gamma annulus" $\beta-\gamma$ coincidence method depicted in Fig. 1a. A partial BGO coincidence shield (not full annulus), covering 0.2π in the downward direction was constructed using 3, 30 mm x 20 mm x 5 mm thick rectangular pieces of BGO, covered in 5 layers of white teflon tape. 2 mm of plastic was used shield the BGO from direct positron irradiation. The partial BGO coincidence "shield" was read out with a separate PMT. This shield was configured around the camera front end, similar to that shown in Fig. 1a. Although non-ideal, this BGO shield was used to demonstrate the high GRB rejection efficiency obtained by requiring a $\beta-\gamma$ coincidence. The β camera and the BGO shield (one end readout by a PMT) were put in coincidence. We will see that with this inefficient, 0.2π prototype coincidence shield, requiring a $\beta-\gamma$ coincidence for every event significantly dropped the sensitivity.

The energy spectrum measured in the CaF_2(Eu) is shown below the image on the far right of Figure 5. We see from both the images and spectra of Figure 5 that the $\beta-\gamma$ coincidence method appears to be at least as efficient (and perhaps better) in restoring the image contrast as the beta shield method. Restoring the image contrast is equivalent to removing the γ ray component and leaving the positron component; compare with the ^{204}Tl image in Figure 4 with no background present. The measured relative β, γ, and $\gamma+\beta$ ray detection rates ratio from the first three images were 1:1.6:2.6, respectively. The γ ray rejection efficiency of this $\beta-\gamma$ coincidence technique was measured to be 98.5% (see end of section II for definition of rejection efficiency). The $\gamma-\gamma$ contribution was < 2% of the $\beta-\gamma$ coincidences. The detected $\beta-\gamma$ coincidence activity rate was a factor of 15 lower than the combined β and γ rates when not in coincidence. This lower rate is consistent with (1) the fact that the partial BGO shield subtended only 0.2π at the center of the CaF_2(Eu) disk, and (2) if a γ ray traversed the BGO shield, the overall probability of interacting was estimated to be in a range between approximately 0.4 and 0.97 for the given geometry..

In Figure 6 we show typical detected digital oscilloscope PMT signals from the CaF_2(Eu)-GSO phoswich detector configuration with ^{18}F as the source of both positrons and annihilation γ rays. The GSO (~ 60 ns decay time) pulse from the PMT has a sharp rise and fall and the CaF_2(Eu) (~1μs decay time) signal has a long tail. In Fig. 6a, we see the slow CaF_2(Eu) decay from a positron hit. Fig. 6b shows only the fast GSO signal from an annihilation γ ray interaction. We chose the criterion that a hit in both the CaF_2(Eu) (slow decay component) and the GSO (fast decay component), with a maximum amplitude greater than 30 mV signified the desired $\beta^+-\gamma$ coincidence event. In Fig. 6c, we show such an event. By triggering on a high leading edge pulse, delaying for 200 ns and setting the linear gate on the slow component, the desired $\beta^+-\gamma$ coincidence events can be identified and used for imaging. The linear gate was set as indicated in Fig. 6c, with roughly 90% the spectrum in Figure 6a passing the gate. This portion of the pulse went into a shaping amplifier and was digitized. The time integrated light yield of CaF_2(Eu) is a factor of 2.5 greater than for GSO.

Figure 7 shows measured energy spectra of ^{18}F in the CaF_2(Eu)-GSO phoswich detector. The delayed linear gate technique successfully discriminates between pure GSO events, pure CaF_2(Eu) events and superimposed events from both scintillators. In (a) both β shielded and unshielded $(\beta+\gamma)$ spectra are shown without any pulse shape discrimination. Note that the pulse height of CaF_2(Eu) is approximately a factor of 2.5 greater than for GSO. In (b) only the slow component (CaF_2(Eu)) of the phoswich signals is integrated and digitized using the delayed linear gate technique. This results in a large reduction of the fast GSO component (γ ray) and enhancement of the CaF_2(Eu) (positron) portion. Here the gate width was set at 1.5μs (200 ns delay). We required that the desired superimposed CaF_2(Eu)-GSO scintillation signals to have a fast and relatively high amplitude leading edge. As expected, the γ/β^+ events ratio in CaF_2(Eu) decreases with increasing leading edge discriminator threshold. For a 50 keV threshold, the dual event (coincidence) phoswich GRB rejection efficiency was measured to be 98.6%. Without coincidence, the detected γ/β rate ratio was 4.8:1. With the coincidence acquisition, the $\gamma-\gamma$ contribution was ~6% of the $\beta-\gamma$ events. In Figure 7c the delay was set to zero, the gate width set to 300 ns, and only the GSO (γ hit) component was integrated and digitized. Note the near absence of the CaF_2(Eu) component.

IV. SUMMARY AND CONCLUSION

We have characterized the annihilation gamma ray background problem for our surgical β ray camera. The extent of the problem depends on how specific the tumor uptake of the chosen radiopharmaceutical. This tumor to normal tissue uptake ratio determines the relative detected rates of β and gamma rays. For a realistic source activity ratio in a simulated tumor and brain phantom, we observed that the annihilation gamma ray background potentially can be a problem for imaging, even in the very thin scintillator used. Fairly complicated images acquired with an β transmission phantom showed a significantly reduced contrast when imaging positrons vs. electrons due to the background annihilation gamma rays randomly interacting within the detector. Two beta-gamma coincidence rejection methods were investigated, both of which were > 95% efficient for gamma ray rejection and which restored image contrast significantly. As with any background removal process, the sensitivity diminished using coincidence acquisition. This reduction is minimized with the use of a highly efficient (geometric and intrinsic) gamma ray absorber. Although the technique was demonstrated with positrons and annihilation GRB, in principle, it may be applied to imaging any radiopharmaceutical beta source that has an associated background ray present. However, because of the collinearity of annihilation gamma rays, the coincidence sensitivity will be the highest for positron imaging.

V. ACKNOWLEDGMENTS

This work was supported in part by grants from the Department of Energy (DE-FCO3-87-ER 60615), National Institutes of Health (R01-CA56655), (RO1-CA61037) and the State of California (IRB-0225).

VI. REFERENCES

[1] B.E. Patt, J.S. Iwanczyk, M.P. Tornai, C.S. Levin, and E.J. Hoffman. Development of a Mercuric Iodide Detector Array for Medical Imaging Applications. *Nucl. Inst. & Meth. A* **366** (1995) 173-182.

[2] L.R. MacDonald, M.P. Tornai, C.S. Levin, J. Park, M. Atac, D.B. Cline, E.J. Hoffman. Investigation of the Physical Aspects of Beta Imaging Probes Using Scintillating Fibers and Visible Light Photon Counters. *IEEE Trans. Nucl. Sci.* **42-4,** August 1995:1351-1357.

[3] L.R. MacDonald, M.P. Tornai, C.S. Levin, J. Park, M. Atac, D.B. Cline, E.J. Hoffman. Small Area, Fiber Coupled Scintillation Camera for Imaging Beta-Ray Distributions Intra-Operatively. In *Photoelectronic Detectors, Cameras and Systems*, Eds. C.B. Johnson, E.J. Fenyves, *Proceedings of the SPIE* **2551** (1995) 92-101.

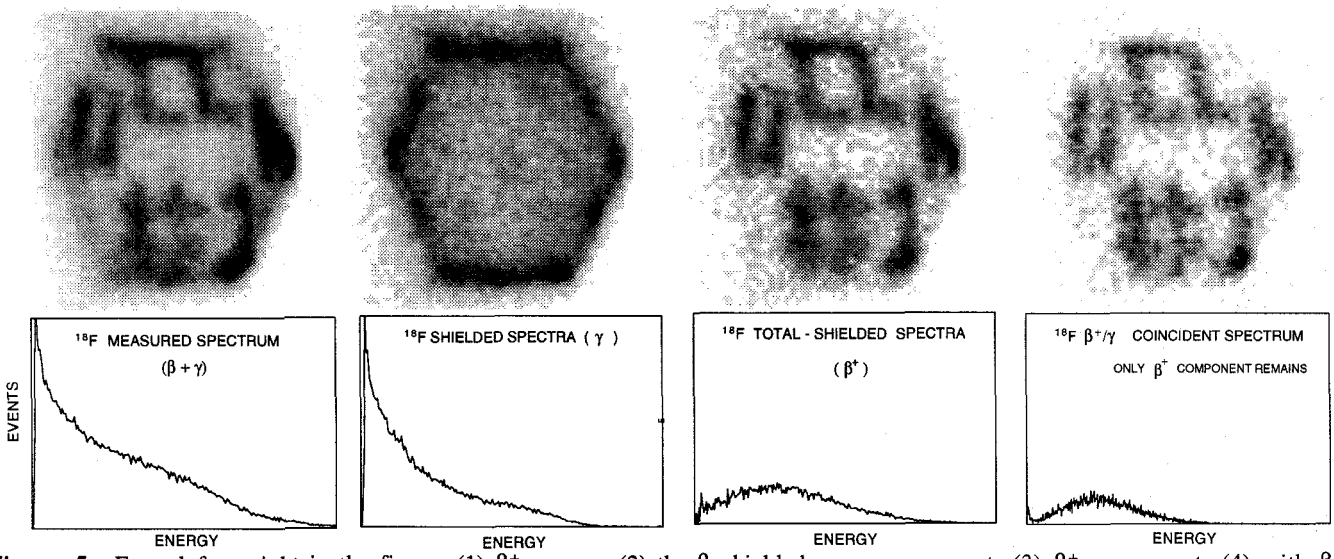

Figure 5. From left to right in the figure: (1) $\beta^+ + \gamma$ ray; (2) the β shielded γ ray component; (3) β^+ component; (4) with $\beta-\gamma$ coincidence using an active BGO shield. The energy spectra measured in the $CaF_2(Eu)$ for each case are shown below the image.

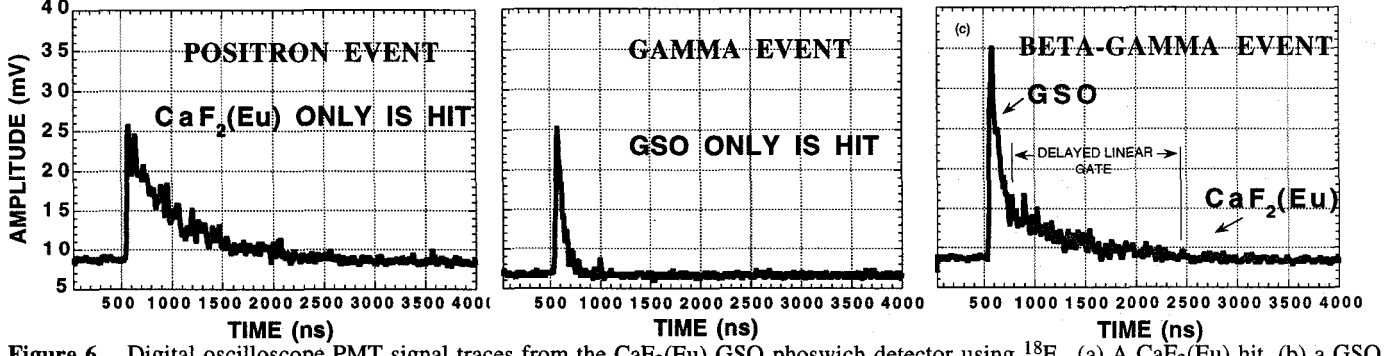

Figure 6. Digital oscilloscope PMT signal traces from the $CaF_2(Eu)$-GSO phoswich detector using ^{18}F. (a) A $CaF_2(Eu)$ hit, (b) a GSO hit (a gamma-ray interaction), (c) A hit in both $CaF_2(Eu)$ and GSO signifies the desired $\beta^+-\gamma$ coincidence.

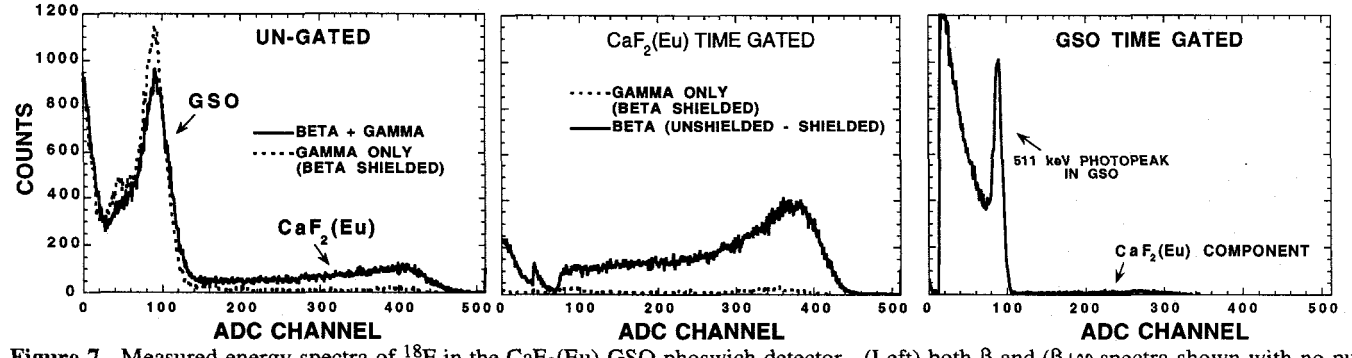

Figure 7. Measured energy spectra of ^{18}F in the $CaF_2(Eu)$-GSO phoswich detector. (Left) both β and $(\beta+\gamma)$ spectra shown with no pulse shape discrimination; (Middle) $CaF_2(Eu)$ component only from the "delayed linear gate" technique, (large reduction GSO component); (Right) the delay was set to zero and only the gamma ray GSO component was integrated and digitized.

[4] C.S. Levin, L.R. MacDonald, M.P. Tornai, E.J. Hoffman, J. Park. Optimizing Light Collection from Thin Scintillators Used in a Beta-Ray Camera for Surgical Use. *IEEE Trans. Nucl. Sci.* **43-3** (1996) 2053-60.

[5] M.P. Tornai, L.R. MacDonald, C.S. Levin, S. Siegel, E.J. Hoffman. Design Considerations and Initial Performance of a 1.2 cm^2 Beta Imaging Intra-Operative Probe. *IEEE Trans. Nucl. Sci.* **43-4**:2326-2335 (August 1996).

[6] M.P. Tornai, E.J. Hoffman, C.S. Levin, L.R. MacDonald. Optimization of Fluor Concentration in a New Organic Scintillator for *In Situ* Beta Imaging. *IEEE Trans. Nucl. Sci.* (1996) (in press).

[7] M.P. Tornai, L.R. MacDonald, C.S. Levin, S. Siegel, E.J. Hoffman, J. Park, M. Atac, D.B. Cline. Miniature Nuclear Emission Imaging System for Intra-operative Applications. In *Proceedings from UCLA International Conference on Imaging Detectors in High Energy & Astroparticle Physics, World Scientific Publishing*, 1996 (in press).

[8] M.P. Tornai, C.S. Levin, L.R. MacDonald, E.J. Hoffman. Investigation of Crystal Geometries for Fiber Coupled Gamma Imaging Intra-operative Probes. Presented in this Conference.

[9] RR Raylman, SJ Fischer, RS Brown, SP Ethier, RL Wahl. ^{18}F-Fluorodeoxyglucose-Guided Breast Cancer Surgery with a Positron-Sensitive Probe: Validation in Preclinical Studies. *J. Nuc. Med.* **36**(10):1869-1874.

[10] F. Daghighian, J.C. Mazziotta, E.J. Hoffman, et. al. Intraoperative Beta Probe: A Device for Detecting Tissue Labeled with Positron or Electron Emitting Isotopes During Surgery. *Med. Phys.* **21**(1): 153-7 (1994).